PHYSICAL REVIEW B **89**, 161405(R) (2014)

Globally enhanced chiral field generation by negative-index metamaterials

SeokJae Yoo,[1] Minhaeng Cho,[2] and Q-Han Park[1,*]

[1]*Department of Physics, Korea University, Seoul 136-713, Korea*

[2]*Department of Chemistry, Korea University, Seoul 136-713, Korea and Korea Basic Science Institute, Seoul 136-713, Korea*

(Received 4 December 2013; revised manuscript received 30 March 2014; published 23 April 2014)

We show that negative-index metamaterials can generate chiral electromagnetic fields, which can be used to enhance molecular chiroptical signals by inducing strong local magnetic fields. Compared to circularly polarized light (CPL), the enhanced chiral field generated by a double-fishnet negative-index metamaterial shows a 3.5-fold enhancement of the volume-averaged optical chirality and possesses the same handedness as that of incident CPL, thereby forming a globally enhanced chiral field. By analyzing near-field configurations, the mechanism of the optical chirality enhancement by double-fishnet negative-index metamaterial is elucidated. We thus anticipate that these metamaterials have potential applications in chiroptical spectroscopy.

DOI: 10.1103/PhysRevB.89.161405 PACS number(s): 78.67.Pt, 33.55.+b, 73.20.Mf, 78.20.Ek

Chiroptical spectroscopy is an efficient optical method used to characterize the absolute configuration of chiral molecules that have nonsuperimposable mirror images. Circular dichroism (CD) measurement, one of the most popular chiroptical methods, utilizes differential absorption of chiral molecules corresponding to two opposite circular polarizations [1]. CD signals, however, are inherently weak because the chiral length scale of molecules is much smaller than that of light and they are about 10^{-6} to 10^{-2} times weaker than absorption. Therefore, amplification of CD signals has been a challenging issue in chiroptical spectroscopy [1,2].

Recently, it has been shown that certain configurations of spatially varying electromagnetic fields, so-called "superchiral" fields in a standing wave form, can enhance dissymmetric CD signals more than circularly polarized light [3–6]. Several groups have also demonstrated that strong near fields in the immediate vicinity of nanostructures generate enhanced chiral fields because locally varying electromagnetic fields can meet the required conditions for enhancements of chiroptical signals [7–12]. For an improved detection of chiral molecules using chiral fields, however, two significant factors should be considered: the achiral design of nanostructures and the globally enhanced chiral field generation. First, it is noted that nanostructures with chiral geometry have their own structural chiral signals [13–15], which could easily contaminate chiral signals from molecules enhanced by the local chiral fields. Although the chiral geometry of nanostructures can generate strong chiral fields at resonant frequency [7,10], it is difficult to distinguish enhanced molecular chiral signals from structural chiral signals in the CD measurements, illustrating the need for an achiral nanostructure for the sensing of chiral molecules with chiral fields. Secondly, locally enhanced chiral field generation [7–10,12] alone cannot provide measurable CD signal enhancement because the measured CD signals result from the overall optical chirality of enhanced chiral fields over the entire region in the vicinity of the nanostructure [11]. In other words, the generation of globally enhanced chiral fields having uniform handedness throughout the volume containing chiral molecules, is desirable for practical chiral molecular sensing. Recently, Garcia-Etxarri and Dionne suggested that surface-enhanced CD measurement is feasible by using high-index nonchiral nanoparticles [11]. However, little has been known for the global enhancement of chiral fields in a large volume region.

In this Rapid Communication, we demonstrate that negative-index metamaterials can generate the significantly enhanced chiral fields upon incidence of circularly polarized light. Inside the cavity of stacked double-fishnet layers (as shown in Fig. 1), the generated chiral fields have the same handedness (either left or right circularly polarized state) over the entire region inside each cavity. Compared with differential absorption, i.e., CD signal, of molecules in circularly polarized plane waves, the double-fishnet negative-index metamaterials enhance differential absorption itself by a factor of 3.5 in volume-average optical chirality. Such an increase in the differential absorption will give rise to measurable enhancement of CD signals. Furthermore, our structure has achiral geometry so as to avoid chiral signals from its own structure. This is absolutely critical in selectively measuring chiroptical signals using such enhanced chiral fields. We also explain herein how achiral negative-index materials can generate the globally enhanced chiral fields via strong excitation of local magnetic fields. To the best of our knowledge, negative-index materials have been considered neither for generating enhanced chiral field nor for characterizing absolute configuration of chiral molecules in those nanostructures.

Recently, as a measure of chirality of electromagnetic wave, the optical chirality (C), which is one of the zilches considered by Lipkin, has been used by Tang and Cohen to characterize the superchiral fields [3], which is defined by Eq. (1):

$$C \equiv -\frac{\varepsilon_0 \omega}{2} \mathrm{Im}[\mathbf{E}^* \cdot \mathbf{B}], \tag{1}$$

where ε_0 is vacuum permittivity and ω is angular frequency, electric field $\mathbf{E}$ and magnetic field $\mathbf{B}$ are complex-valued vectors, and the asterisk denotes complex conjugation. The differential absorption, i.e., CD signal, is directly proportional to the optical chirality as $\Delta A = A_L - A_R = 4G''C/\varepsilon_0$, where A_L (A_R) represents the absorbance of chiral molecules for left (right) CPL, and G'' is the imaginary part of the isotropic electric-magnetic dipole polarizability of a given chiral molecule [8]. From Eq. (1), we note that spatially

*Corresponding author: qpark@korea.ac.kr

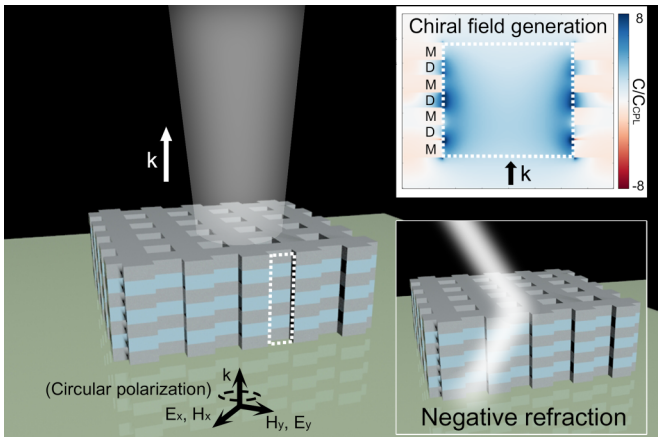

FIG. 1. (Color online) Schematic of a double-fishnet structure generating globally enhanced chiral fields. The upper inset shows a spatial distribution of the optical chirality under normally incident left CPL. Globally enhanced chiral fields are generated inside the cavities of a double-fishnet structure. Double-fishnet structure also causes negative refraction of light.

varying electric and magnetic fields, which are parallel and out of phase to each other, have nonvanishing optical chirality C. Throughout this Rapid Communication, we shall consider the ratio C/C_{CPL}, where C_{CPL} represents the optical chirality of CPL, i.e., $C_{\mathrm{CPL}} = \varepsilon_0 \omega E_0^2/c$ with E_0 and c being the amplitude and the speed of light, respectively.

Here, we consider negative-index metamaterials for the generation of enhanced chiral fields. Negative-index metamaterials have strong local magnetic responses and near fields excited by their structure. Therefore, we expect that negative-index metamaterials can efficiently generate enhanced chiral fields, as optical chirality is proportional to magnetic field amplitude in Eq. (1). In this work, we consider the so-called double-fishnet structure as a representative case of negative-index metamaterial. Double-fishnet structures have been used to obtain optical magnetism and negative refractive indices at various wavelength bands [16–22]. Double-fishnet structures comprise metal-dielectric-metal (MDM) multilayers with square cavities, as shown in Fig. 1. Our double-fishnet structure is composed of 30-nm silver layers and 35-nm hydrogen silsesquioxane (HSQ) layers on the glass substrate. The material parameters for silver are obtained from the reported data [23], and the refractive index of HSQ and glass are 1.41 and 1.5, respectively [18]. Cavities are square shaped with sides $h_x = h_y = h = 200$ nm, and located periodically with lattice constants $a_x = a_y = a = 320$ nm. This double-fishnet structure has recently been shown to be a low-loss negative-index metamaterial [18]. Given that the basic unit of a double-fishnet structure consists of a single MDM layer, we investigated numerically the enhanced chiral field generation with single (MDM), double [$(MD)_2M$], and triple layers [$(MD)_3M$].

Direct evidence of the chiral field generation by the negative-index metamaterial can be found in Fig. 2. Figure 2(a) and the inset of Fig. 2(b) show spectra of transmittance and effective parameters for the metamaterial under left circularly polarized incident light, respectively. Figure 2(a) shows two

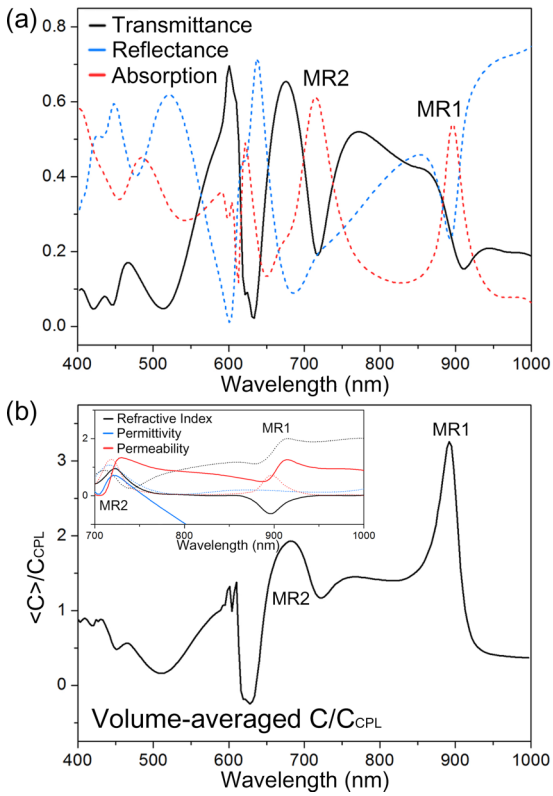

FIG. 2. (Color online) (a) Spectra for transmittance, reflectance, and absorption of a single MDM double-fishnet structure. (b) Volume-averaged optical chirality inside the cavities of the double-fishnet structure, which is normalized by the optical chirality of incident circularly polarized plane wave C_{CPL}. MR1 and MR2 indicate the first- and second-order magnetic resonances, respectively. Inset of (b): Retrieved effective parameters for the double-fishnet structure (solid and dashed lines denote the real and imaginary parts, respectively).

absorption peaks at 714-nm and 894-nm wavelengths, which also correspond to two transmittance dips. Effective permeability in the inset of Fig. 2(b) indicates that the absorption peaks at 894 and 714 nm originate from the first- and second-order magnetic resonances, respectively. The two magnetic resonances are related to the surface plasmon polariton (SPP) Bloch modes satisfying the phase matching conditions of the wave vectors to the periodicity of cavities [19]. The first- and second-order SPP Bloch modes correspond to the $\Gamma - X$ and $\Gamma - M$ directions of the Brillouin zone, respectively. It is known that these two Bloch modes form gap SPPs in between two metal layers [17–19]. The gap SPPs of the two Bloch modes circulate inside an MDM layer, and provide optical magnetic resonance and negative effective permeability [24]. Effective permittivity, which describes an electric response, is highly negative at the long wavelength region supported by the cutoff frequency of cavities. From these effective parameters, we can expect that simultaneous excitations of strong electric and magnetic fields occur at two magnetic resonance wavelengths.

In order to verify our expectation that the negative-index property is of use to generate enhanced chiral field, we compared the spectra of volume-averaged optical chirality inside cavities and the spectral positions of magnetic resonances. As can be seen in Fig. 2(b), the two major peaks of

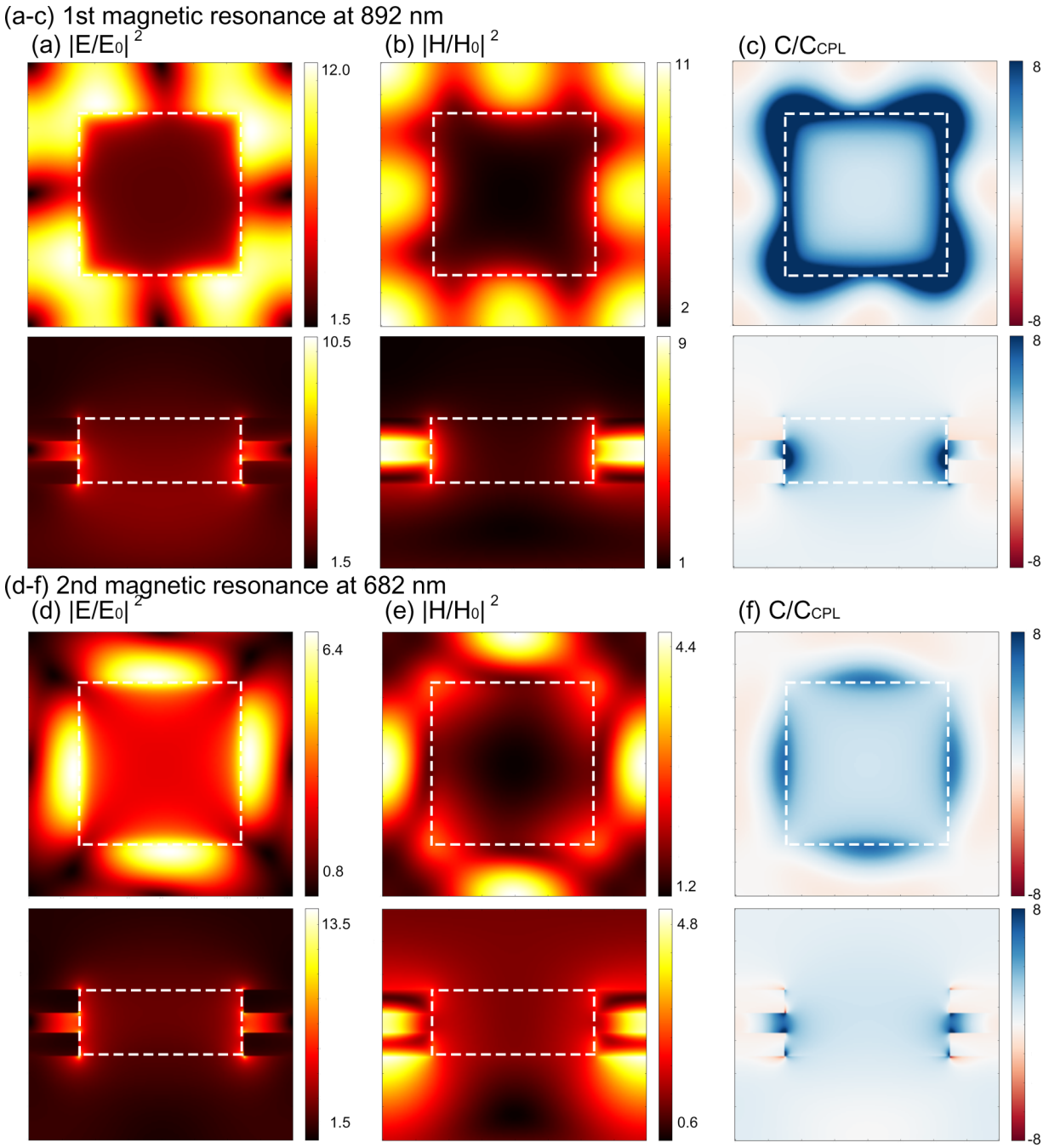

FIG. 3. (Color online) Horizontal and vertical distribution of electric fields, magnetic fields, and optical chirality ratio C/C_{CPL} at (a)–(c) first-order magnetic resonance near 892 nm and (d)–(f) second-order magnetic resonance near 682 nm. White dotted lines indicate the cavity boundaries in the double-fishnet structure.

volume-averaged optical chirality and those of the imaginary part of effective permeability appear at the same wavelengths (682 and 892 nm, respectively.) Thus, it is concluded that the absorbed energy, shown as a red line in Fig. 2(a), is used to form gap SPPs inside metamaterial structures, which subsequently generate the significantly enhanced chiral fields, as shown in Fig. 2(b). Likewise, Fig. 2(a) shows that high reflectance (at 637 nm) results in the optical chirality dip at the same wavelength. This is due to the fact that most of the incident light is reflected back, and thus optical chirality is reduced inside the metamaterial.

In order to investigate the origin of the enhanced chiral field generation by the double-fishnet structure, we analyzed near-field responses of electromagnetic fields and the optical chirality at two magnetic resonances. Figure 3 illustrates horizontal distributions of fields at the central dielectric gap, vertical distributions of electric fields, and the optical chirality ratio C/C_{CPL}. Vertical distributions show that the major enhancement of the optical chirality occurs at the dielectric gap where gap SPPs are formed. Figures 4(a) and 4(b) clearly show that there are strong enhancements in longitudinal electric and magnetic fields near cavity edges. Strong E_z

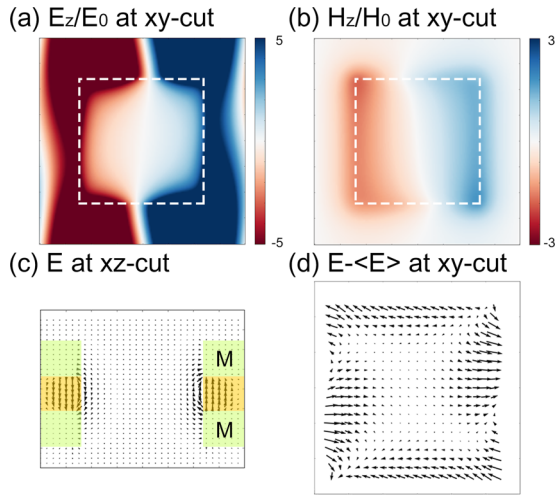

FIG. 4. (Color online) Time snapshots of longitudinal (a) electric field E_z/E_0 and (b) magnetic field H_z/H_0 at xy cut (white lines specify cavity boundaries), (c) vector field maps of electric field vector $\mathbf{E} = E_x\hat{\mathbf{x}} + E_z\hat{\mathbf{z}}$ at xz cut (green-yellow-green region indicates metal-dielectric-metal layers), and (d) differential electric field vector $\mathbf{E} - \langle\mathbf{E}\rangle = (E_x - \langle E_x\rangle)\hat{\mathbf{x}} + (E_y - \langle E_y\rangle)\hat{\mathbf{y}}$ inside cavities at xy cut. The wavelength of the field map in (a)–(d) is 892 nm, which is the first-order magnetic resonance.

originates from excited gap SPPs forming virtual currents between two metal layers [see Fig. 4(c)], and then induces strong resonance of transverse magnetic field components (H_x, H_y) providing effective permeability (μ) responses at the far-field level. In contrast, transverse electric components supported by cavities (E_x, E_y), providing effective permittivity (ε) responses, induce H_z because they have a spatial curl of electric fields. Figure 4(d) displays the differential electric field vector $\mathbf{E} - \langle\mathbf{E}\rangle = (E_x - \langle E_x\rangle)\hat{\mathbf{x}} + (E_y - \langle E_y\rangle)\hat{\mathbf{y}}$ that induces the longitudinal magnetic field component H_z. When the longitudinal components E_z and H_z are dominant and out of phase with respect to each other, optical chirality in Eq. (1) becomes strongly enhanced. This explains the mechanism of enhanced chiral field generation by the negative-index metamaterial. The mechanism shown here differs from the conventional mechanism based on geometrical chirality of nanostructure, which already gives a curl of electric fields at the curvature of chiral nanostructures [7,8,10,12]. Our mechanism therefore presents a new route to generate superchiral fields using an *achiral* nanostructure.

Another noteworthy feature is that the generated enhanced chiral field is global inside the cavity, meaning that the chiral handedness is spatially uniform [Figs. 3(c) and 3(f)]. From Eq. (1), we find that optical chirality can be positive or negative, and that most nanostructures previously sutdied generate superchiral fields with varying handedness flipping signs [7,9,10,12]; this is detrimental to volume-averaged enhancement over the entire region. Therefore, the globally enhanced chiral fields seen in Figs. 3(c) and 3(f) result in the volume-averaged enhancement of the optical chirality [see Fig. 2(c)]. Thus, the present enhanced chiral field generation method will be of critical use in practical molecular sensing because CD signals from net molecules are measured inside the nanostructures.

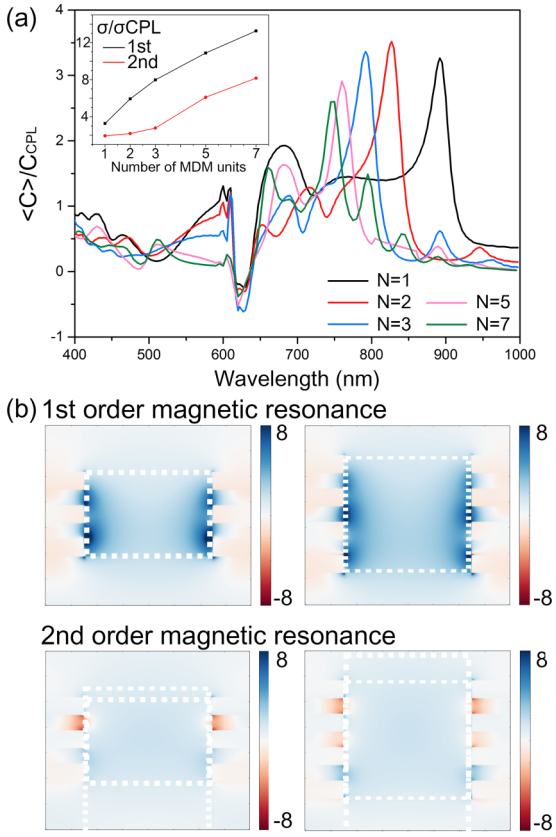

FIG. 5. (Color online) (a) Volume-averaged optical chirality. Inset of (a): Differential absorption of net molecules inside cavities (σ) at two resonances. The normalizing unit (σ_{CPL}) is the differential absorption of molecules, by incident CPL, within the volume of a single MDM cavity. (c) The xz cut of optical chirality for double (left) and triple units (right) at the first-order resonance (upper) and the second-order resonance (bottom).

Finally, comparing the spatial distribution of the optical chirality in Figs. 3(c) and 3(f), the first-order magnetic resonance (892 nm) generates stronger enhancement of the local optical chirality than the second-order magnetic resonance (682 nm) does. This explains why the volume-averaged optical chirality of the first-order magnetic resonance is much higher than that of the second-order magnetic resonance in Fig. 2(b).

With this in mind, one important question remains: Can stacking MDM layers of the double-fishnet structure enlarge enhanced optical chiral regions inside cavities with the same handedness? As shown in Fig. 5, we considered stacked layers $[(\mathrm{MD})_n\mathrm{M}]$ up to $n = 7$. In metamaterial studies, it has been demonstrated that effective parameters and metamaterial figures of merit are influenced by the number of stacking layers [19,21,22]. Figure 5(a) shows that the *volume-averaged* enhancement factor of optical chirality at the first-order (but not at the second-order) magnetic resonance remains the same even with increasing the number of MDM units. In the inset of Fig. 5(a), the differential absorption of net molecules inside cavities, $\sigma \equiv \int \Delta A\, dV$, which is directly related to the strength of CD signals, clearly shows that the first-order resonance is much more efficient for the enhanced chiral field generation than the second-order resonance, because

the differential absorption of net molecules inside cavities at the first-resonance wavelength increases linearly relative to the number of MDM units. This peculiar observation can be understood by examining the vertical distribution of the optical chirality [Fig. 5(b)]. In Fig. 5(b), there are changes in the handedness of chiral fields produced by the second-order magnetic resonance mode. In contrast, the distribution of the optical chirality at the first-order resonance shows highly uniform optical chirality enhancement without sign flipping. From this observation, we can conclude that the globally enhanced chiral fields can be attained only for the first-order magnetic resonance when the number of MDM units increases. The seven layers in Fig. 5, amounts to a physical path length of 0.5 μm in CD measurement, while the effective path length, taking into account the enhanced chirality by a factor of 3, is about 1.5 μm. Effective path lengths can be further increased by adding more layers or using optimally designed metamaterials to improve the sensitivity of detecting chiral molecules.

The spectral shift of the generated enhanced chiral fields is also noteworthy. In Fig. 5(a), the volume-averaged optical chirality at two magnetic resonances changes as the number of stacking layers increases. This is a natural consequence of metamaterials having tunable characteristics. Metamaterial studies have shown that spectral position and strength of magnetic resonance can be tuned by simply controlling the number of stacking layers, cavity size, and periodicity [18–22]. Likewise, we expect that such factors, which tune the optical properties of metamaterials, can affect the spectral position and strength of the enhanced chiral fields. This is particularly important because one can easily make metamaterials suitable for a given chiral molecule. However, there could be potential complications originating from calibration of measured spectrum and specific interaction of chiral molecules with metamaterial.

In this study, we have shown that negative-index metamaterials can be used to generate the enhanced chiral fields. The underlying mechanism of the enhanced chiral field generation by negative-index metamaterials is shown to be directly related to the simultaneous excitation of strong electric and magnetic fields in the longitudinal direction, satisfying the parallel and out-of-phase condition for large optical chirality in Eq. (1). The present study and results can provide guidelines for achieving strongly enhanced chiral field generation by specifically designed *nonchiral* structures. The enhanced chiral field generated by the metamaterials would be of use in chiroptical spectroscopy. We anticipate that the bridging of chiroptical spectroscopy and photonic metamaterials, two distinct disciplines of optics, will offer new possibilities for applications of metamaterials in the future.

This research was supported by Nano-Material Technology Development Program through the National Research Foundation of Korea (NRF) funded by The Ministry of Science, ICT & Future Planning (MSIP) (Grants No. 2009-0082665 and No. 2011-0020205). This work was also supported by the National Research Foundation of Korea (NRF) grant funded by the Korea government (MSIP) (Grant No. 2009-0092831). M.C. is grateful for financial support from NRF (Granta No. 20110010033 and No. 2013013156).

[1] L. D. Barron, *Molecular Light Scattering and Optical Activity*, 2nd ed. (Cambridge University Press, Cambridge, UK, 2004).
[2] H. Rhee, J. S. Choi, D. J. Starling, J. C. Howelld, and M. Cho, Chem. Sci. **4**, 4107 (2013).
[3] Y. Tang and A. E. Cohen, Phys. Rev. Lett. **104**, 163901 (2010).
[4] Y. Tang and A. E. Cohen, Science **332**, 333 (2011).
[5] J. S. Choi and M. Cho, Phys. Rev. A **86**, 063834 (2012).
[6] K. Y. Bliokh and F. Nori, Phys. Rev. A **83**, 021803 (2011).
[7] E. Hendry, T. Carpy, J. Johnston, M. Popland, R. V. Mikhaylovskiy, A. J. Lapthorn, S. M. Kelly, L. D. Barron, N. Gadegaard, and M. Kadodwala, Nat. Nanotechnol. **5**, 783 (2010).
[8] E. Hendry, R. V. Mikhaylovskiy, L. D. Barron, M. Kadodwala, and T. J. Davis, Nano Lett. **12**, 3640 (2012).
[9] M. Schäferling, X. Yin, and H. Giessen, Opt. Express **20**, 26326 (2012).
[10] M. Schäferling, D. Dregely, M. Hentschel, and H. Giessen, Phys. Rev. X **2**, 031010 (2012).
[11] A. García-Etxarri and J. A. Dionne, Phys. Rev. B **87**, 235409 (2013).
[12] T. J. Davis and E. Hendry, Phys. Rev. B **87**, 085405 (2013).
[13] D. L. Jaggard, A. R. Mickelson, and C. H. Papas, Appl. Phys. **18**, 211 (1979).
[14] S. S. Oh, A. Demetriadou, S. Wuestner, and O. Hess, Adv. Mater. **25**, 612 (2013).
[15] A. Guerrero-Martínez, B. Auguié, J. L. Alonso-Gómez, Z. Džolić, S. Gómez-Graña, M. Žinić, M. M. Cid, and L. M. Liz-Marzán, Angew. Chem., Int. Ed. Engl. **50**, 5499 (2011).
[16] G. Dolling, M. Wegener, C. M. Soukoulis, and S. Linden, Opt. Lett. **32**, 53 (2007).
[17] R. Ortuño, C. García-Meca, F. J. Rodríguez-Fortuño, J. Martí, and A. Martínez, Phys. Rev. B **79**, 075425 (2009).
[18] C. García-Meca, J. Hurtado, J. Martí, A. Martínez, W. Dickson, and A. Zayats, Phys. Rev. Lett. **106**, 067402 (2011).
[19] C. García-Meca, R. Ortuño, F. J. Rodríguez-Fortuño, J. Martí, and A. Martínez, Opt. Lett. **34**, 1603 (2009).
[20] J. Yang, C. Sauvan, H. Liu, and P. Lalanne, Phys. Rev. Lett. **107**, 043903 (2011).
[21] S. Zhang, W. Fan, N. C. Panoiu, K. J. Malloy, R. M. Osgood, and S. R. Brueck, Opt. Express **14**, 6778 (2006).
[22] J. Valentine, S. Zhang, T. Zentgraf, E. Ulin-Avila, D. A. Genov, G. Bartal, and X. Zhang, Nature (London) **455**, 376 (2008).
[23] E. D. Palik, *Handbook of Optical Constants of Solids* (Academic, New York, 1997).
[24] In the inset of Fig. 2(a), the effective permeability does not reach to the negative value strictly at magnetic resonance for the single MDM layer but it does for stacked MDM layers [18]. However, this distinction is irrelevant for our purpose and we use the term negative permeability without such distinction.